JOURNAL OF Materials CHEMISTRY

In situ Raman spectroscopic studies of trimethylindium pyrolysis in an OMVPE reactor

Chinho Park,*[a] Woo-Sik Jung,[a] Zhisong Huang[b] and Timothy J. Anderson[c]

[a]*School of Chemical Engineering and Technology, Yeungnam University, 712-749 Gyongsan, Korea. E-mail: chpark@yu.ac.kr*
[b]*Lam Research Corp, Fremont, California 94538-6470, USA*
[c]*Department of Chemical Engineering, University of Florida, Gainesville, FL 32611-6005, USA. E-mail: tim@nersp.nerdc.ufl.edu*

Received 21st August 2001, Accepted 9th October 2001
First published as an Advance Article on the web 12th December 2001

An *in situ* investigation of thermal decomposition reactions of trimethylindium (TMIn) in a vertical, upflow chemical vapor deposition reactor has been carried out using Raman spectroscopy. Monomethylindium (MMIn) and atomic indium were detected along with the precursor TMIn using N_2 as the carrier gas. Atomic indium was identified by the peak at 2215 cm^{-1}, which is equal to the difference between two spin–orbit split levels of atomic indium in the ground electronic state. The multiple peaks corresponding to MMIn, which were enhanced by a resonance Raman effect, consisted of fundamentals($\nu_2 = 1097$ cm^{-1},$\nu_3 = 430$ cm^{-1},$\nu_5 = 1364$ cm^{-1}, $\nu_6 = 696$ cm^{-1}) and a high progression of overtones and combination bands. Concentration profiles were obtained from the measurements of peak intensities of TMIn, MMIn, and indium at different distances away from the hot susceptor along the vertical centerline of the reactor.

Introduction

Organometallic vapor phase epitaxy (OMVPE) is a proven technique for the deposition of compound semiconductor thin films for solid state device applications.[1] The development of realistic reactor models that describe the spatial dependence of growth rate and film composition is valuable for optimizing reactor designs, establishing suitable growth conditions, and interpreting experimental results. The robustness of such models is usually limited by uncertainties in reaction mechanisms and their rate constants.[1–3] A prerequisite for specifying reaction mechanisms is the identification and characterization of reaction intermediates. The intermediates typically encountered in OMVPE of compound semiconductors are usually unstable and present at very low concentrations that vary with position in the reactor. One approach has been to use *ex situ* sampling techniques to obtain qualitative and quantitative information on intermediates.[3] Such techniques usually are not suitable for identifying reactant and short-lived intermediates at low concentrations since parasitic reactions, long sample transit times, and flow perturbations by the sample probe can occur. In general nonperturbative, *in situ* probes have been more successful in detecting the intermediates. Raman scattering, IR-diode laser absorption, UV absorption, laser induced fluorescence (LIF), and coherent anti-Stokes Raman scattering (CARS) have all been used to study OMVPE chemistries.[4] *In situ* probes can also be used to improve the controllability of OMVPE process in commercial reactors.

Although Raman spectroscopy can detect most chemical species and has high spatial resolution, there have been a limited number of studies of organometallic decomposition reactions, because of its relatively low detection sensitivity.[5–7] It is noted, however, that the detection sensitivity limitation is relaxed in special cases by resonance Raman scattering. When the wavelength of the excitation light is close to or in resonance with an available excited state of a chemical species, the scattering cross-section is significantly enhanced by the resonance Raman effect (RRE), making it possible to detect the species at very low concentrations.[8] In a sense, resonance Raman scattering is complementary to resonance fluorescence since it is applicable to a species having a low fluorescence quantum yield.

TMIn is the most commonly used precursor for OMVPE deposition of indium-containing compound semiconductors. The pyrolysis reaction of TMIn was first investigated in a toluene carrier by Jacko and Price[9] as early as 1964. The pyrolysis reaction was proposed to consist of three consecutive homolytic fission steps:

$$(CH_3)_3In \rightarrow (CH_3)_2In + CH_3 \quad (1)$$

$$(CH_3)_2In \rightarrow CH_3In + CH_3 \quad (2)$$

$$CH_3In \rightarrow In + CH_3 \quad (3)$$

According to their kinetic study, reactions (1) and (2) occur almost simultaneously yielding monomethylindium (MMIn) as a reaction intermediate, which was suggested to be relatively stable at a temperature lower than 480 °C. At higher temperature, reaction (3) proceeds to yield atomic indium as one of the final reaction products. Other studies have been directed at identifying reaction products in the decomposition of TMIn in various ambients.[9–13] The principal hydrocarbon products were found to be C_2H_6 and CH_4,[9–11] and methyl radicals were also observed at very low concentration using *in situ* IR-diode laser spectroscopy.[11] Haigh and O'Brien[12] failed to observe the existence of atomic indium using atomic absorption spectroscopy and concluded that reaction (3) takes place only heterogeneously. Hebner and Killeen,[13] however, observed atomic indium in a H_2 carrier using resonance fluorescence spectroscopy.

In this study *in situ* Raman spectroscopy was used to identify reactive intermediates and to measure their relative concentrations during thermal decomposition of trimethylindium (TMIn) in an OMVPE reactor. This study is part of a more comprehensive investigation of the reaction mechanisms important in OMVPE growth of indium-containing compound

 DOI: 10.1039/b107586a

semiconductors, including InGaN which is an important material for green and blue light-emitting diodes.[14]

Experimental

The apparatus used in the present study consists of a laser Raman spectrometer coupled to a custom upflow OMVPE reactor system, which has been described previously.[15] Nitrogen was selected as a carrier gas, because it has a strong vibrational Raman band which is used to normalize the peaks of reactive species. Raman spectra were measured along the vertical centerline of the reactor in the carrier gas. The temperature distribution within the reactor was determined by purely rotational bands of N_2 molecules.[7] The relative mole fraction of each gas-phase chemical species in the reactor was obtained from the ratio of integrated intensity of the primary peak of the In species (478 cm^{-1} for TMIn, 430 cm^{-1} for MMIn, and 2215 cm^{-1} for atomic In) to that for the N–N stretch at 2331 cm^{-1} of the N_2 carrier gas. Since the carrier gas was in large excess, its mole fraction was approximately unity and hence assumed constant throughout the reactor. For the present study, the operating pressure of the reactor was maintained at atmospheric pressure. The N_2 carrier gas was UHP nitrogen (Liquid Air, Inc.), and the TMIn source (Texas Alkyls) was electronic grade.

Results and discussion

Raman spectra in the frequency range 250 to 3000 cm^{-1} were recorded by probing a small volume element in the OMVPE reactor. The peak observed at 2331 cm^{-1}, which corresponds to vibration of the N_2 carrier molecules, was used as an absolute frequency calibration. Fig. 1(a) shows the spectrum which was recorded by probing a region very close to the inlet. Decomposition of TMIn was not expected at this location because of low local gas phase temperature (*ca.* 70 °C). As previously reported,[15] the Raman spectrum of gas-phase TMIn consists of four main spectral features: a broad transition at 113 cm^{-1} corresponding to the in-plane bending vibration of InC_3 skeleton, a sharp transition at 478 cm^{-1} overlapping with a very broad transition near 500 cm^{-1} (corresponding to a symmetric and asymmetric stretching of the InC_3 skeleton, respectively), a sharp transition at 1173 cm^{-1} associated with C–H bending of the methyl groups, and a peak at 2925 cm^{-1} which is associated with C–H stretching vibrations of the methyl groups. These transitions are easily found in the spectrum of Fig. 1(a), except for the 113 cm^{-1} transition, which overlaps with the rotational transitions of the carrier N_2 molecules and is not displayed here.

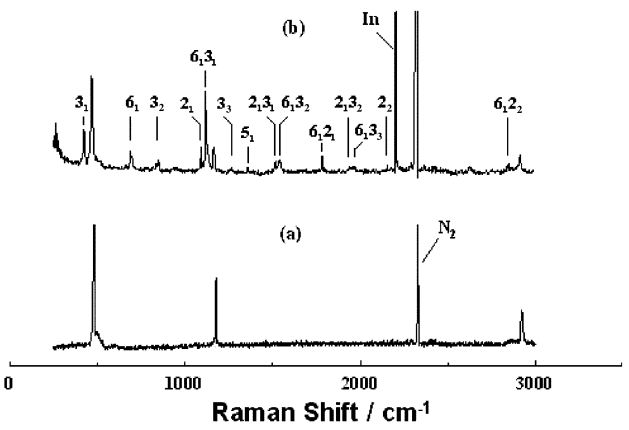

Fig. 1 Raman spectra of the $(CH_3)_3In/N_2$ mixture at 70 °C (a) and 300 °C (b). The excitation wavelength was 488.0 nm. The peak at 2331 cm^{-1} correponds to the vibration of N_2 carrier molecules.

Fig. 1(b) shows the spectrum which was taken by probing a hotter region (*ca.* 300 °C) 3.4 mm away from the heated susceptor where TMIn molecules were partially decomposed. In addition to peaks corresponding to TMIn, there are several peaks in the spectrum apparently associated with some intermediates and/or end products of the decomposition reactions of TMIn. The additional peaks can not be attributed to simple hydrocarbon species[9–11] such as CH_3, CH_4 and C_2H_6 which are known to be products of TMIn pyrolysis.[16,17] It is evident, therefore, that the hydrocarbon species were formed below the detection limit of Raman scattering and the additional peaks are attributed to indium-bearing species such as dimethylindium (DMIn), MMIn, and atomic indium. DMIn, however, is not believed to be responsible for the observed additional peaks for several reasons. First, the concentration of DMIn is expected to be much lower than that of MMIn.[9] Assuming that DMIn has the same linear structure as $(CH_3)_2In^+$,[18] its symmetric In–C stretching band would be much more intense than the other fundamental vibration bands, as shown in Raman spectra of $(CH_3)_2In^+$,[18] $(CH_3)_2Zn$,[19] and $(CH_3)_2Cd$.[19] Furthermore, the In–C stretching frequency (430 cm^{-1}) in Fig. 1(b) is relatively low for the symmetric metal–C mode of dimethylmetal compounds.[19] As a result, the additional peaks in Fig. 1(b) are believed to correspond to MMIn and atomic indium.

The very strong peak observed at 2215 cm^{-1} in Fig. 1(b) is assigned to an electronic Raman scattering transition between the two spin–orbit split levels ($^2P_{1/2}$ and $^2P_{3/2}$) of atomic indium in the ground electronic state ($5s^25p^1$). Using the atomic indium absorption spectrum given by Candler,[20] the splitting between these two levels was calculated to be 2214 cm^{-1}, after wavelength correction using the index of refraction of air. This assignment is also supported by the facts that the line width was instrumental-limited, characteristic of an atomic transition and the frequency shift of the peak was independent of the excitation wavelength. Hebner and Killeen[13] also observed atomic indium in the pyrolysis of TMIn in a H_2 carrier using *in situ* resonance fluorescence spectroscopy.

The peaks other than those corresponding to TMIn and indium in Fig. 1(b) are likely attributable to vibrations of MMIn. Although the concentration of MMIn was expected to be comparable to or lower than those of the hydrocarbon products, its vibrational peaks were observed because the Raman scattering cross-sections were significantly enhanced by the RRE. The effect is observed when the frequency of the excitation light is very close to or lies within the range of an electronic absorption by MMIn.[8] There is, to date, no report on the UV–visible electronic absorption spectrum of MMIn, but it may be deduced from the spectrum[21] of its cognate, monomethylgallium (MMGa). Assuming that the spectra of MMGa and MMIn show similarities as do the spectra of GaH and InH, the maximum absorption wavelength of MMIn is expected to be *ca.* 418 nm, and corresponds to that of MMGa (386 nm).[21] The difference is taken by comparing the difference of the $A\,^1\Pi$ ($v=0$)–$X\,^1\Sigma^+$ ($v=0$) transition in the spectra of GaH and InH which occur at 422 and 454 nm,[22] respectively. Therefore, the excitation wavelength of 488.0 nm used in Fig. 1(b) is at slightly longer wavelengths than the absorption maximum of MMIn. In contrast to the normal (nonresonance) Raman spectrum, the resonance Raman spectrum has several characteristic features.[8] Two of them, namely the appearance of a high overtone and combination progression of some fundamental frequencies and the dependence of band intensities on the excitation wavelength, were observed in Raman spectra of MMIn (see below).

Assuming C_{3v} equilibrium symmetry for MMIn, there are six vibrational modes, three totally symmetric (a_1) and three doubly degenerate (e) modes, all of which are Raman active. The a_1 modes consist of a symmetric C–H stretch (v_1), symmetric CH_3 deformation (v_2), and In–C stretching (v_3), while

the e modes are comprised of an asymmetric C–H stretching (ν_4), asymmetric CH_3 deformation (ν_5), and CH_3 rocking (ν_6). Fig. 1(b) shows that there are more peaks than expected for the normal Raman spectrum of MMIn. This suggests that the spectrum shown in Fig. 1(b) represents the resonance Raman spectrum and the peaks other than the fundamentals are overtones and combination bands.

Based on the spectrum shown in Fig. 1(b), four of the six fundamental vibrational modes were assigned frequencies. The intense peak at 430 cm^{-1} is attributed to the In–C stretch. This frequency, ν_3, is lower than the In–C vibration frequency (478 cm^{-1}) in TMIn owing to the stronger In–C bond strength.[9] Methyl groups bound to a single metal atom in $(CH_3)_nM$ ($n>1$) type compounds typically have metal–methyl vibrations in the 450 to 650 cm^{-1} range.[19] Monomethylmetal organometallic compounds, however, have lower reported metal–methyl vibration. For example, the metal–methyl vibration frequency for CH_3Zn and CH_3Cd have measured value of 445 and 356 cm^{-1}, respectively, as determined by fluorescence spectroscopy.[23] The peak at 696 cm^{-1} corresponds to the rocking mode (ν_6) of a methyl group. The vibration frequency is compared with the values 687 and 725 cm^{-1} observed in the gas-phase TMIn infrared spectrum[24] and is very similar to the value 690 cm^{-1} of MMGa adsorbed on the GaAs(100) surface as measured by high-resolution electron energy loss spectroscopy (HREELS).[25] The peaks at 1097 and 1364 cm^{-1} are assigned to the symmetric (ν_2) and asymmetric (ν_5) C–H bending vibrations, respectively. The ν_2 and ν_5 vibration frequencies fall into the frequency ranges found for organometallic compounds with terminal methyl groups[19] and the ν_2 frequency is comparable to those of CH_3Zn (1064 cm^{-1}) and CH_3Cd (1000 cm^{-1}).[23] Two C–H stretching bands (ν_1 and ν_4) were too weak to be observed or overlapped with the C–H stretching band of TMIn. Recently Himmel *et al.*[26] measured IR spectra of MMIn in an Ar matrix and assigned vibrational frequencies of its ν_2, ν_3, and ν_5 modes, which are in good agreement with our Raman data, but their theoretical frequency (533.1 cm^{-1}) of the ν_6 mode which was absent in IR absorption is considerably different from our experimental frequency (696 cm^{-1}).

The remaining peaks are overtones of ν_2 and ν_3, and combination bands such as $\nu_2+n\nu_3$ ($2_1 3_n$), $\nu_6+n\nu_2$ ($6_1 2_n$), and $\nu_6+n\nu_3$ ($6_1 3_n$). It is noteworthy that, in agreement with theory,[27] only the fully symmetric fundamental displays the RRE. Similar to the spectrum reported for CH_3I, the combination $\nu_6+\nu_3$ peak intensity for MMIn is greater than their fundamentals.[28] A summary of peak assignments is given in Table 1.

Characteristic of overtone vibrational transitions, the frequency intervals (430, 424 and 419 cm^{-1}) between successive transitions of the $n\nu_3$ (3_n) progression are nearly equal but decrease with increasing quantum number due to anharmonicity. It is possible to estimate the In–C bond dissociation energy in MMIn from the anharmonicity. Assuming that the In–C interaction potential can be approximated by the standard Morse potential,[29] the frequency intervals between successive transitions in the progression are approximated by $\Delta\nu(v)\cong\omega_e-\omega_e\chi_e(2v+1)$, where v is the vibrational quantum number, ω_e the fundamental frequency, and $\omega_e\chi_e$ the anharmonicity. From the frequency values given in Table 1, it can be shown that $\omega_e\cong 433$ cm^{-1} and $\omega_e\chi_e\cong 3$ cm^{-1} for the ν_3 vibration. An upper limit for the In–C bond dissociation energy (D_e) in MMIn can be estimated to be $D_e\cong\omega_e^2/4\omega_e\chi_e\cong 188.3$ kJ mol^{-1}. Although there is considerable uncertainty in the value of the anharmonicity $\omega_e\chi_e$ resulting from uncertainties in the frequency determination of the transitions, this estimated value of the bond dissociation energy is close to the experimental value (170.3 kJ mol^{-1}) reported by Jacko and Price.[9]

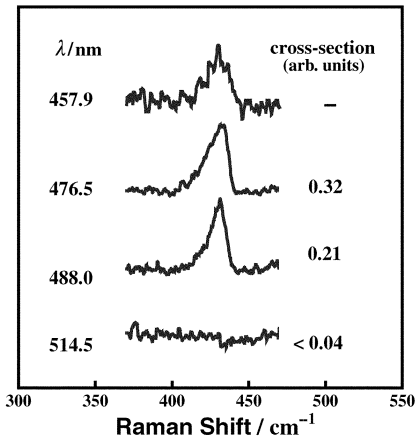

Fig. 2 Variations of the ν_3 peak and its relative scattering cross-section of CH_3In at several different excitation wavelengths.

Fig. 2 shows the excitation wavelength dependence of the intensity and relative Raman scattering cross-section of the ν_3 peak at 430 cm^{-1}. The relative scattering cross-section can be obtained by measuring the integrated intensity of the ν_3 peak at various excitation wavelengths under the same reactor conditions and normalizing it with that of the N_2 vibrational transition at 2331 cm^{-1} recorded at the same scan. Since the carrier N_2 molecules were in large excess and thus considered to be at constant concentration, normalization to its vibrational transition cancels possible variations in excitation laser power and the scattering light detection efficiency. Reliable values were obtained for excitations of 476.5 and 488.0 nm. When exciting with a wavelength of 514.5 nm, however, the scattering transitions associated with MMIn were not observable and an upper limit was estimated from the noise level. The value at the 457.9 nm excitation was not reliable because of a poor signal-to-noise ratio and hence is not listed in Fig. 2. Although limited wavelengths were studied, the enhancement

Table 1 Raman bands of CH_3In and their assignments

Fundamental		Overtone		Combination	
Assignment	Frequency/cm^{-1}	Assignment	Frequency/cm^{-1}	Assignment	Frequency/cm^{-1}
ν_1 (1_1)	Not observed				
ν_2 (2_1)	1097	$2\nu_1$ (2_2)	2178	$\nu+\nu_2$ ($6_1 2_1$)	1790
				$\nu+2\nu_2$ ($6_1 2_2$)	2856
ν_3 (3_1)	430	$2\nu_3$ (3_2)	854	$\nu_2+\nu_3$ ($2_1 3_1$)	1524
		$3\nu_3$ (3_3)	1273	$\nu_2+2\nu_3$ ($2_1 3_2$)	1954
				$\nu_6+\nu_3$ ($6_1 3_1$)	1124
				$\nu_6+2\nu_3$ ($6_1 3_2$)	1547
				$\nu_6+3\nu_3$ ($6_1 3_3$)	1975
ν_4 (4_1)	Not observed				
ν_5 (5_1)	1364				
ν_6 (6_1)	696				

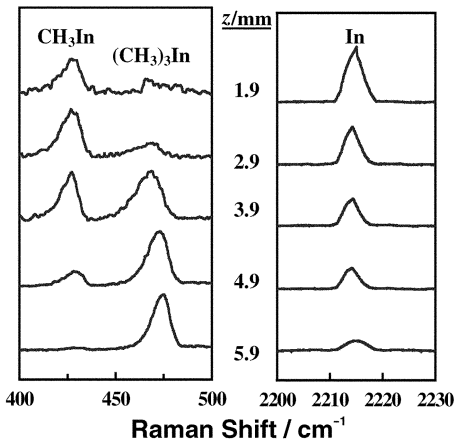

Fig. 3 Intensity variations of Raman scattering transitions for $(CH_3)_3In$, CH_3In, and indium along the vertical centerline of the reactor in thermal decompositions of $(CH_3)_3In$. The distance below the surface of the heated susceptor is designated as z.

factor is likely to increase with slightly decreasing the wavelength below 476.5 nm.

The centerline concentration profiles of TMIn, MMIn, and indium were determined by measuring their Raman scattering transition intensities. An example of the measurement is illustrated in Fig. 3, which displays the variation of intensities at different distances away from the susceptor along the centerline of the reactor. The transitions at 430, 478, and 2215 cm^{-1} were used to monitor the concentrations of MMIn, TMIn, and indium, respectively. To measure the concentration of each species, each integrated intensity was divided by that of the carrier N_2 vibration at 2331 cm^{-1}. The normalized intensity provides a measure of the absolute mole fraction for TMIn, which can be calculated from its vapor pressure at the source temperature. For the case of MMIn and indium, it provides a measure of the relative mole fractions since their Raman scattering cross-sections are unknown. Fig. 4 shows concentration profiles of TMIn, MMIn, and indium along the centerline of the reactor. The TMIn precursor began to decompose at *ca.* 220 °C. The concentrations of TMIn and indium were found to decrease and increase monotonically toward the solid/gas interface, respectively. On the other hand, the MMIn species was observed at the threshold of the TMIn

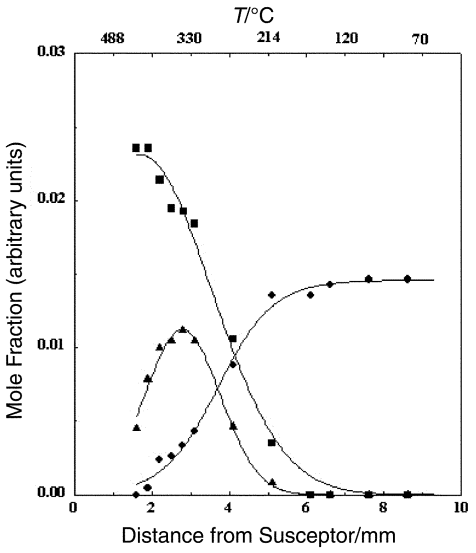

Fig. 4 Concentration profiles of $(CH_3)_3In$ (●), CH_3In (▲), and indium (■) along the vertical centerline of the reactor in thermal decompositions of $(CH_3)_3In$. The mole fraction for TMIn is absolute, and the mole fractions for MMIn and In are relative. Lines shown in the figure are the spline interpolation of data.

decomposition and its concentration reaches a maximum at the distance approximately 2.9 mm away from the susceptor. The latter observation indicates that the TMIn thermal decomposition is mostly homogeneous under the current reactor conditions, in agreement with the results in decomposition in a He carrier.[10]

It should be pointed out that particle formation in the immediate vicinity of the susceptor was observed as evidenced by the presence of strong scattering of excitation laser light. The particle formation was observable only in the region where significant TMIn decomposition occurred. The particle may be indium liquid droplets, which are formed by the condensation of gas-phase indium produced as a result of TMIn decomposition. This is not surprising considering the fact that an equilibrium vapor pressure of indium is very low under our experimental conditions (for example, $P = 7.9 \times 10^{-8}$ Torr at 527 °C).

Conclusion

An analysis of *in situ* Raman spectra in the pyrolysis of TMIn in a N_2 carrier gas showed that TMIn, MMIn and atomic indium are present in the reaction zone of the OMVPE reactor. This is the first time that MMIn has been identified by *in situ* Raman spectroscopy. The concentration distributions of these species were also measured and the results indicated that while TMIn precursor is depleted before reaching the susceptor surface in the gas phase, both MMIn and indium are present in the gas/solid interface. Based on the results obtained in this study, a thorough investigation is under way to study the homogeneous reaction mechanisms of the InGaN OMVPE in N_2 and/or H_2 environment.

Acknowledgements

The authors would like to thank Mr Pete Axson for his technical assistance. This research was supported in part by the Yeungnam University Research Grants in 1998.

References

1 G. B. Stringfellow, *Organometallic Vapor Phase epitaxy: Theory and Practice*, Academic Press, Boston, 1989.
2 K. F. Jensen, *J. Cryst. Growth*, 1989, **98**, 1483.
3 P. Zanella, G. Rossetto, N. Brianese, F. Ossola, M. Porchia and J. O. Williams, *Chem. Mater.*, 1991, **3**, 225.
4 W. Richter, P. Kurpas, R. Lückerath, M. Motzkus and M. Waschbüsch, *J. Cryst. Growth*, 1991, **107**, 13.
5 T. O. Sedgwick and J. E. Smith Jr, *J. Electrochem. Soc.*, 1976, **123**, 254.
6 Y. Monteil, P. Favre, P. Raffin, J. Bouix, M. Vaille and P. Gibart, *J. Cryst. Growth*, 1988, **93**, 159.
7 Y. Monteil, P. Favre, A. Bekkaoui, P. Raffin, J. Bouix, J. Marcillat and P. Dutto, *J. Cryst. Growth*, 1988, **93**, 270.
8 D. L. Rousseau, J. M. Friedman and P. F. Williams, in *Raman Spectroscopy of Gases and Liquids*, ed. A. Weber, Springer-Verlag, New York, 1979.
9 M. G. Jacko and S. J. W. Price, *Can. J. Chem.*, 1964, **42**, 1198.
10 N. I. Buchan, C. A. Larsen and G. B. Stringfellow, *J. Cryst. Growth*, 1988, **92**, 591.
11 J. E. Butler, N. Bottka, R. S. Sillmon and D. K. Gaskill, *J. Cryst. Growth*, 1986, **77**, 163.
12 J. Haigh and S. O'Brien, *J. Cryst. Growth*, 1984, **67**, 75.
13 G. A. Hebner and K. P. Killeen, *J. Appl. Phys.*, 1990, **67**, 1598.
14 S. Nakamura, *Solid State Commun.*, 1997, **102**, 237.
15 Z. Huang, C. Park and T. J. Anderson, *J. Organomet. Chem.*, 1993, **449**, 77.
16 B. Schrader, *Raman/Infrared Atlas of Organic Compounds*, VCH Publishers, New York, 2nd edn., 1989.
17 M. E. Jacox, *J. Phys. Chem. Ref. Data*, 1984, **13**, 45.
18 C. W. Hobbs and R. S. Tobias, *Inorg. Chem.*, 1970, **9**, 1998.
19 E. Maslowsky Jr, *Vibrational Spectra of Organometallic Compounds*, Wiley, New York, 1977.

20 C. Candler, *Atomic Spectra and the Vector Model*, Van Nostrand, Princeton, NJ, 1964.
21 K. P. Killeen, *Appl. Phys. Lett.*, 1992, **61**, 1864.
22 K. P. Huber and G. Herzberg, *Molecular Spectra and Molecular Structure, Vol. IV: Constants of Diatomic Molecules*, Van Nostrand, New York, 1979.
23 E. S. J. Robles, A. M. Ellis and T. A. Miller, *Chem. Phys. Lett.*, 1991, **178**, 185.
24 J. R. Hall, L. A. Woodward and E. A. V. Ebsworth, *Spectrochim. Acta*, 1964, **20**, 1249.
25 X.-Y. Zhu, J. M. White and J. R. Creighton, *J. Vac. Sci. Technol. A*, 1992, **10**, 316.
26 H.-J. Himmel, A. J. Downs, T. M. Greene and L. Andrews, *Chem. Commun.*, 1999, 2243.
27 L. A. Nafie, P. Stein and W. L. Peticolas, *Chem. Phys. Lett.*, 1971, **12**, 131.
28 F. Marbel and A. B. Meyer, *J. Chem. Phys.*, 1993, **98**, 21.
29 J. M. Hollas, *High Resolution Spectroscopy*, Butterworth, London, 1982.